Journal of Clinical and Translational Hepatology **2023**
DOI: 10.14218/JCTH.2022.00062

Original Article

Single-cell RNA-seq Revealed that Altered Tumor Infiltrating Lymphocytes in Cirrhotic Liver Indicate Development of Hepatocellular Carcinoma

Jingxian Duan[1#], Peng Zhu[2#], Yong Zhang[3#], Tianhao Mu[1,4], Yingqiang Li[4], Rui Xiong[5], Su Chen[2], Yingmei Li[4], Zhicheng Li[1], Shifu Chen[1,4] and Lei Zhang[2,6,7*]

[1]Shenzhen Institutes of Advanced Technology, Chinese Academy of Sciences, Shenzhen, Guangdong, China; [2]Hepatic Surgery Center, Tongji Hospital, Huazhong University of Science and Technology, Wuhan, Hubei, China; [3]Department of Hepatobiliary Surgery, Union Hospital, Tongji Medical College, Huazhong University of Science and Technology, Wuhan, Hubei, China; [4]HaploX Biotechnology Co. Ltd, Shenzhen, Guangdong, China; [5]Hepatopancreatobiliary Surgery, Hubei Cancer Hospital, Wuhan, Hubei, China; [6]Department of Hepatobiliary Surgery, Shanxi Bethune Hospital, Shanxi Academy of Medical Sciences, Shanxi Medical University, Shanxi Tongji Hospital, Tongji Medical College, Huazhong University of Science and Technology, Taiyuan, Shanxi, China; [7]Key Laboratory of Hepatobiliary and Pancreatic Diseases of Shanxi Province(Preparatory), Shanxi Bethune Hospital, Shanxi Academy of Medical Sciences, Shanxi Medical University, Shanxi Tongji Hospital, Tongji Medical College, Huazhong University of Science and Technology, Taiyuan, Shanxi, China

Received: 14 October 2022 | **Revised:** 13 December 2022 | **Accepted:** 18 January 2023 | **Published online:** 16 March 2023

Abstract

Background and Aims: Cirrhosis is the precursor lesion for most hepatocellular carcinoma (HCC) cases. However, no biomarker effectively predicted HCC initiation before diagnosis by imaging. We aimed to investigate the hallmarks of immune microenvironments in healthy, cirrhotic livers and HCC tumor tissues and to identify immune biomarkers of cirrhosis-HCC transition. ***Methods:*** Expression matrices of single-cell RNA sequencing studies were downloaded and integrated with Seurat package vignettes. Clustering was performed to analyze the immune cell compositions of different sample types. ***Results:*** The cirrhotic liver and HCC tumors had distinct immune microenvironments, but the immune landscape of cirrhotic livers was not markedly modified compared with healthy livers. Two subsets of B cells and three subsets of T cells were identified in the samples. Among the T cells, naïve T cells were more prominent in the cirrhotic and healthy liver samples than in the HCC samples. In contrast, the neutrophil count was lower in cirrhotic livers. Two macrophage clusters were identified, one that actively interacted with T cells and B cells and was enriched in cirrhotic blood compared with HCC blood samples. ***Conclusions:*** Decreased naïve T cell infiltration and increased neutrophil infiltration in the liver may indicate the development of HCC in cirrhotic patients. Alterations in blood-resident immune cells may also be a sign of HCC development in cirrhotic patients. The dynamics of the immune cell subsets may serve as novel biomarkers to predict the transition from cirrhosis to HCC.

Citation of this article: Duan J, Zhu P, Zhang Y, Mu T, Li Y, Xiong R, *et al*. Single-cell RNA-seq Revealed that Altered Tumor Infiltrating Lymphocytes in Cirrhotic Liver Indicate Development of Hepatocellular Carcinoma. J Clin Transl Hepatol 2023. doi: 10.14218/JCTH.2022.00062.

Introduction

Liver cancer is the seventh most common and second most lethal cancer globally, hepatocellular carcinoma (HCC) accounts for 75–85% of liver cancer cases.[1] Cirrhosis is an independent risk factor and has prognostic implication for HCC,[2] regular surveillance is recommended to cirrhotic patients for the early screening of HCC. The progression of cirrhosis involves telomere dysfunction, cellular senescence, inflammatory responses, and Epithelial-mesenchymal transition. At molecular level, aberrant modulations of the Wnt, RAS, JAK/STAT, and p53 pathways were frequently observed.[3] Previous studies identified differentially expressed genes (DEGs) by comparing sequencing data acquired from cirrhotic patients and HCC patients. They were enriched in pathways for cell-cycle, DNA replication, drug metabolism, and p53 signaling.[4,5] It was also reported that the mutation landscape of cirrhotic patients differed from that of HCC patients, and that mutations at key loci including the TERT

Keywords: Immune microenvironment; Single-cell RNA sequencing; Cirrhosis; Hepatocellular carcinoma; Liver.

Abbreviations: ALD, alcoholic liver disease; CMV, cytomegalovirus; DC, dendritic cell; DEG, differentially expressed gene; EBV, Epstein-Barr virus; GEO, gene expression omnibus; GO, gene ontology; HCC, hepatocellular carcinoma; KEGG, kyoto encyclopedia of genes and genomes; NAFLD, nonalcoholic fatty liver disease; NK, natural killer; PBC, primary biliary cholangitis; scRNAseq, single-cell RNA sequencing; tSNE, t-distributed stochastic neighbor embedding; UMAP, uniform manifold approximation and projection.

[#]Contributed equally to this work.

[*]**Correspondence to:** Lei Zhang, Tongji Hospital, Tongji Medical College, Huazhong University of Science and Technology, Wuhan, China; Shanxi Bethune Hospital, Shanxi Academy of Medical Sciences, Shanxi Medical University; Shanxi Tongji Hospital, Tongji Medical College, Huazhong University of Science and Technology, Taiyuan, Shanxi 030032, China. ORCID: https://orcid.org/0000-0002-2227-0613. Tel: +86-13886171160, Fax: 86-27-83662851, E-Mail: zhangl@tjh.tjmu.edu.cn

promoter were indicators of malignant transformation.[6] The transformations at genomic and transcriptomic level can be used to predict the transition from cirrhosis to HCC. Moreover, changes in the local immune landscape were also expected during this malignant transformation, which requires further investigation.

Single-cell RNA sequencing (scRNAseq) has characterized the immune microenvironment of healthy and diseased liver. Several subtypes of T cells, B cells, and unknown subtypes of endothelial cells, Kupffer cells, and hepatocytes were identified in healthy liver samples.[7] Apart from conventional tumor-associated macrophages, a unique cluster of LAMP3$^+$ dendritic cells (DCs) were identified in immune-related ligands of HCC patients, and were proposed to regulate various lymphocytes.[8] Changes in infiltrating immune cells and their regulations during the transformation from healthy liver cells to cells with chronic inflammation and eventually HCCs might determine the response to immunotherapy. Therefore, the aim of the study is to investigate the change of immune cell composition from healthy liver, cirrhotic liver to HCC, and interpret the clinical impacts of the altered immune microenvironment.

Methods

Data collection

Expression matrices of scRNAseq studies were downloaded from the Gene Expression Omnibus (GEO) database. Sequencing results of liver cells extracted from healthy individuals were acquired from GSE115469,[9] GSE136103,[10] and GSE124395.[7] Data of cirrhotic liver cells and circulating tumor cells were obtained from GSE136103.[10] Tissues were collected from cirrhotic patients undergoing orthotropic liver transplantation. Expression matrices of hepatic tumor cells were downloaded from GSE124395[7] and GSE107747.[11] Data of circulating tumor cells extracted from HCC patients were obtained from HRA000069[12] and GSE136103.[10] Data of circulating cells extracted from blood samples of healthy individuals were acquired from SRP073767.[13] The number of cells extracted from each study and the pathological conditions of the samples can be found in Table 1.

Data integration and analysis

Data sequenced with different methods and platforms were integrated with standard Seurat package vignettes.[14] Batch effects were removed; quality control and data normalization were performed as per instruction. Clustering was performed by standard Seurat package vignettes. The number of dimensions representing each cell was reduced by principal component analysis, which contributed to the identification of clusters.

DEGs in clusters were computed, and the clusters were visualized by *t*-distributed stochastic neighbor embedding (tSNE) and uniform manifold approximation and projection (UMAP). The type of cells contained in each cluster was identified manually based on canonical and known markers of immune cells and hepatocytes. Unique immune cell subtypes expressed in healthy liver, cirrhotic liver, and HCC cells were detected by the stimulated vs control PBMCs vignette of Seurat. Hallmark immune cell subtypes expressed in healthy liver, cirrhotic liver, and HCC cells were defined based on the results.[15] SingleR was also used for cluster annotation.[16] Genes with $\log_2$ fold change >1 and adjusted *p*-values <0.05 were assigned as differentially expressed. Gene Ontology (GO), Kyoto Encyclopedia of Genes and Genomes (KEGG) enrichment analysis, and the visualization of DEGs was implemented by the clusterProfiler R package.[17–19] Cell-cell communication analysis was performed with the CellChat R package.[20]

Statistical analysis

Statistical analysis for Figures 1–4 was performed using GraphPad Prism v8.0. The statistical comparison methods are described in the figure captions.

Results

Immune cell composition of cirrhotic samples resembles that of healthy but not HCC samples

We downloaded scRNAseq data that composed of the RNA expression matrices of 142600 cells extracted from 41 individuals in six studies (GSE115469, GSE136103, GSE124395, HRA000069, GSE107747, SRP073767; Table 1). The cells clustered to 20 discrete cell populations that were characterized by differential gene expression (Fig. 5A–C and Supplementary Fig. 1). These cell clusters were annotated as immune cells, hepatocytes, stromal cells (endothelial cells and fibroblasts), and mixed clusters based on the expression of gene markers (Fig. 5D, E). Considering that some of the included studies conducted flow cytometry to select immune cells, the immune cell populations are more prevalent in the integrated dataset. Among immune cells, T cells, natural killer (NK) cells, neutrophils and macrophages are relatively abundant (Fig. 5F). The cluster T cell, T cell 2, and naïve T cell account for 1.57%, 9.09% and 6.38% of the total cell count. NK and NK 2 cluster attributed to 7.41% and 5.52% of the total count respectively. 8.7% cells are macrophages and monocytes. Neutrophil, one of the most abundant types of white blood cells in the blood stream, made up 8.08% of the entire population.

Healthy liver, cirrhotic liver and HCC had varied immune cell composition (Fig. 6A–F). The composition of immune cells in cirrhotic samples was similar to that of the healthy liver samples, with T cells, and NK cells being the prevalent immune cell types. Notably, the immune cell composition of HCC samples was significantly altered compared to the healthy and cirrhotic samples (Fig. 6F). The proportion of NK cells decreased, the abundance of different T cell populations was altered, and neutrophils were evidently more enriched. Comparing blood samples and tissue samples of cirrhosis individuals, neutrophils were dominant in the blood samples as expected, accounting for 14.85% of the cells in the cirrhotic blood sample. In the HCC blood sample, the proportion of neutrophils doubled to 29.05%, indicating an elevated inflammatory response. In healthy blood samples, only B cells, plasma B cells, T cells, NK cells, DCs, macrophages, monocytes, and megakaryocytes were identified (Supplementary Fig. 2). Neutrophils were not identified, possibly due to limitations of the sequencing technique and cell degradation caused by sample handling. Therefore, we excluded healthy blood samples from our downstream analysis.

B cells were more abundant in blood samples of HCC patients compared to cirrhotic patients

We identified two B-cell populations and three T cell populations. CD19-expressing B-cell populations were identified as B cell and plasma B cells based on the genetic markers acquired from published studies,[7–9,21–25] public databases,[26,27] and SingleR.[16] Cluster 12 is a B-cell population with strong expression of MS4A1, CD79A, and BANK1, whereas the expression of DERL3, JCHAIN, and MZB1 was limited. In con-

Table 1. Sample information and cell counts of healthy liver tissues, cirrhotic liver tissues, HCC tissues, HCC blood samples, and cirrhotic blood samples

Dataset ID	Healthy blood	Cirrhotic blood	HCC blood	Healthy liver	Cirrhotic liver	Tumor	Row total
SRP073767	2,899						2,899
	7,767						7,767
	9,517						9,517
HRA000069			45			93	138
			134			116	250
			487			391	878
			503			672	1,175
			380			610	990
			583			540	1,123
GSE136103		8,882					8,882
		6,600					6,600
		8,120					8,120
		7,031					7,031
					4,882		4,882
					6,482		6,482
					5,064		5,064
					4,784		4,784
					2,892		2,892
				2,842			2,842
				1,1179			1,1179
				7,176			7,176
				8,074			8,074
				5,075			5,075
GSE107747			2,949				2,949
			6,917				6,917
GSE124395						387	387
						279	279
						294	294
				1,427			1,427
				1,082			1,082
				1,081			1,081
				1,769			1,769
				454			454
				1,613			1,613
				704			704
				1,385			1,385
GSE115469				1,068			1,068
				1,219			1,219
				3,127			3,127
				1,321			1,321
				1,704			1,704
Column Total	20,183	30,633	11,998	52,300	24,104	3,382	142,600

Study ID and pathological conditions of the samples are shown in Table 1. Each row represents one sample. The numbers in each cell indicates the number of cells extracted from the corresponding sample. HCC, hepatocellular carcinoma.

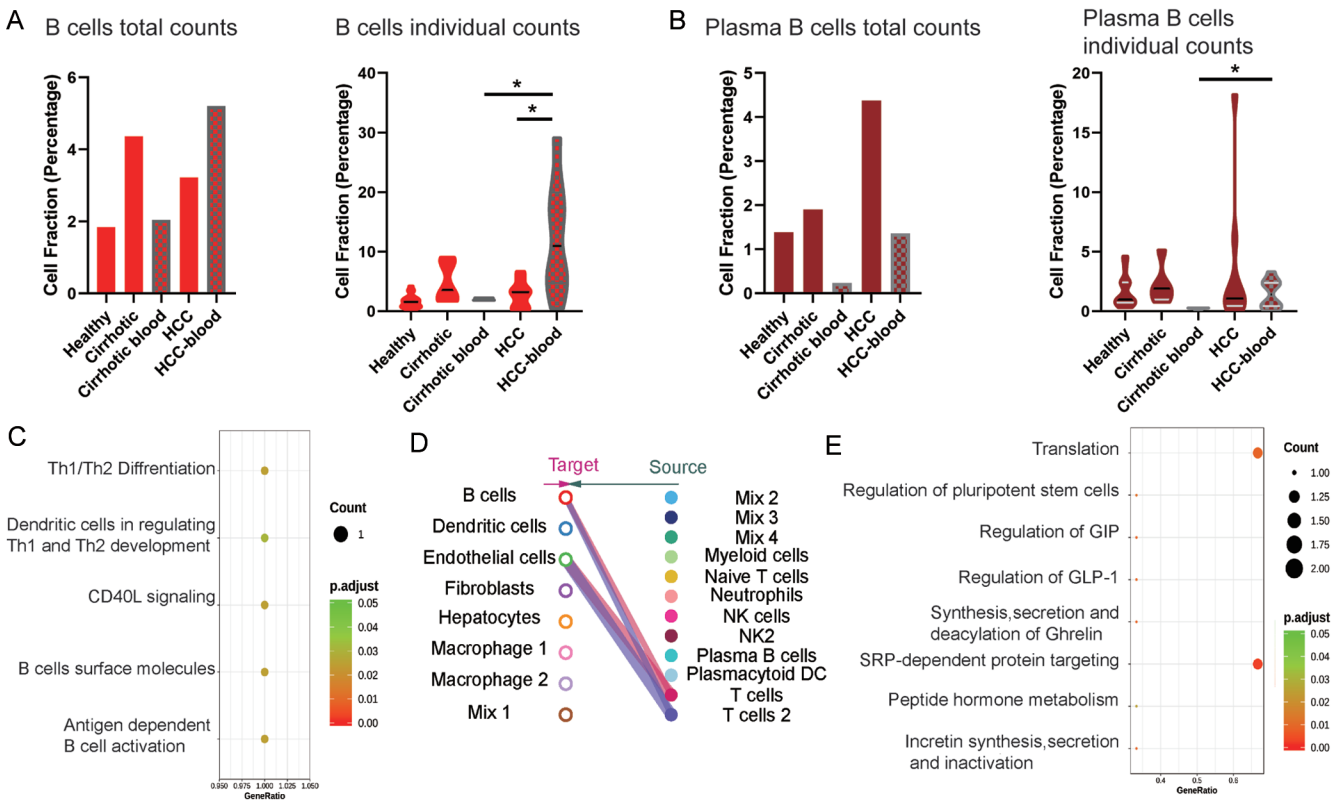

Fig. 1. Subsets of B cells were more enriched in hepatocellular carcinoma blood samples than in cirrhotic blood samples. (A) Percentages of B cells in healthy liver samples, cirrhotic liver samples, cirrhotic blood samples, hepatocellular carcinoma (HCC) tissue samples, and HCC blood samples were calculated. The bar chart (left panel) shows the percentage of B cells in all cells (all patients pooled). The violin plot (right) shows the percentage of B cells in each patient. The shape of the violin plot indicates the distribution of data points, lines denote mean and interquartile range. Significant difference was determined by *t*-test or Wilcoxon's test depending on the results of normality and F tests. ***$p<0.001$, **$p<0.01$, *$p<0.05$, ns, not significant ($p>0.05$). (B) As in (A), but for plasma B cells. (C) Enrichment analysis showing the pathways and cell functions impacted by the DE genes of the B cell cluster. (D) Hierarchical plot shows the inferred intercellular communication network for CD40 signaling. Circle size is proportional to the number of cells in each cell group and edge width shows the communication probability. (E) Enrichment analysis showing the pathways and cell functions impacted by the DE genes of the plasma B cell cluster.

trast, cluster 18 is a subset of B cells that highly expressed DERL3, JCHAIN, SDC1, and MZB1, but without the expression of MS4A1 and BANK1. MS4A1 encodes for the B-lymphocyte surface antigen CD20, whereas JCHAIN, and MZB1 coded proteins are functionally related to immunoglobulin heavy and light chains. Given the above, we postulated that cluster 12 comprised antigen-inexperienced B cells, and cluster 18 contained differentiated plasma B cells that resided in the liver tissue.

We also compared the cell fraction of the two B-cell populations in healthy, cirrhotic, and cancerous samples (Fig. 1A, B). Both the total count (Fig. 1A left panel) and statistical comparison based on individual sample counts (Fig. 1A right panel) were displayed. The B-cell population accounted for 12.47±3.42% of total cell counts in HCC blood samples, significantly higher than that of the cirrhotic blood sample (2.04±0.10%). In fact, this B-cell population was also more enriched in the HCC blood sample than in the HCC tissue sample. No difference was observed at tissue level, showing B-cell abundance was modulated for peripheral immunity. The top DEGs were primarily involved in TH1/TH2 differentiation, DCs regulation TH1/TH2 development, and CD40L signaling (Fig. 1C). T cells interacted with the B cells by CD40 signal modulation (Fig. 2D).

Similar to B cells, plasma B cells accounted for 1.48±0.43% of total cells in HCC blood samples, significantly higher than the composition of plasma B cells in cirrhotic blood samples (Fig. 1B). The plasma B cells were not active for T cell-related cellular process. Instead, they were primarily responsible for protein translation and cotranslational protein targeting to membranes (Fig. 1E). Collectively, the observations indicate that T-helper cells, antigen-inexperienced B cells, and differentiated plasma B cells responsible for antibody secretion were more abundant in HCC blood samples.

Naïve T cells were enriched in cirrhotic tissue samples, but were depleted in HCC tissue samples

Three T cell subsets were identified by high PTPRC (protein alias CD45) and CD3 expression. Cluster 7 was likely a naïve T cell and memory T cell subset because of the increased expression of CCR7. The abundance of this T cell subset was significantly lower in HCC tissue samples (1.23±0.41%) compared with healthy (2.95±0.51%) and cirrhotic liver tissues (4.48±1.11%; Fig. 2A). In addition, naïve T cells and memory T cells were significantly more enriched in blood samples than in tissue samples. Those cells were active in protein translation (Fig. 2B).

Expression of CD3E, CD2, CD7, CD69, and CD4 was enriched in cluster 16, which was believed to be another T cell subset. This T cell population was more abundant in HCC tissue than in other tissue samples (Fig. 2C). It also accounted for 2.11±0.22% of cirrhotic blood cells, significantly higher

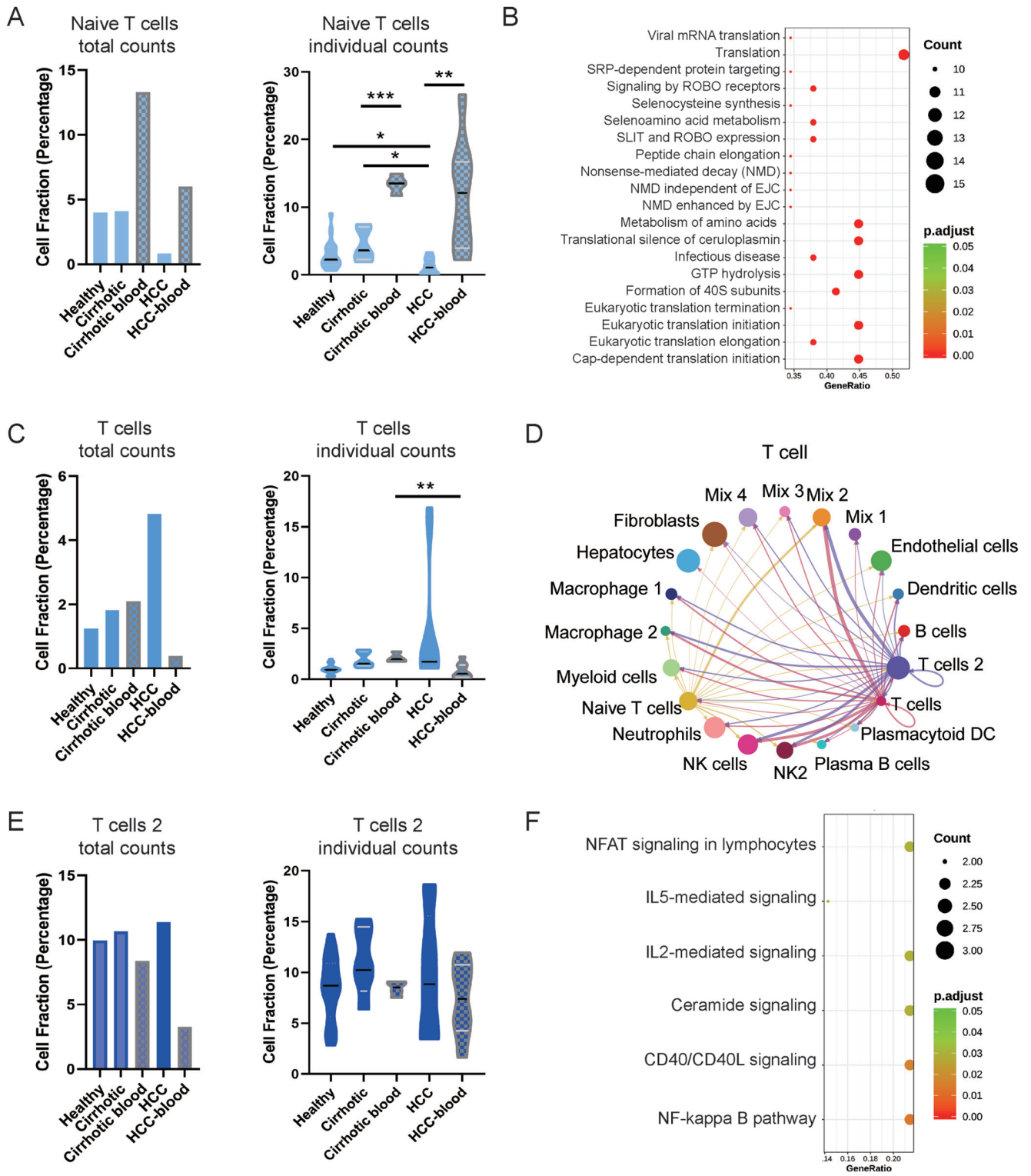

Fig. 2. Subsets of T cells were differentially distributed in cirrhotic samples and hepatocellular carcinoma samples. (A) Percentages of naïve T cells in healthy liver samples, cirrhotic liver samples, cirrhotic blood samples, hepatocellular carcinoma (HCC) tissue samples, and HCC blood samples were calculated. The bar chart (left panel) shows the percentage of T cells in all cells (all patients pooled). The violin plot (right) shows the percentage of T cells in each patient. The shape of the violin plot indicates the distribution of data points, lines denote mean and interquartile range. Significance was determined by *t*-test or Wilcoxon's test depending on the results of normality tests and F tests. ***$p<0.001$, **$p<0.01$, *$p<0.05$, ns, not significant ($p>0.05$). (B) Enrichment analysis showing the pathways and cell functions impacted by the DE genes of the naïve T cells. (C) As in (A), but for T cells. (D) Cell interaction plot shows the inferred probability of interaction between the three subsets of T cells and other cells. The probability was proportional to the width of the lines joining the two types of cells. (E) As in (A), but for T-cell 2. (F) As in (B), but for T-cell 2.

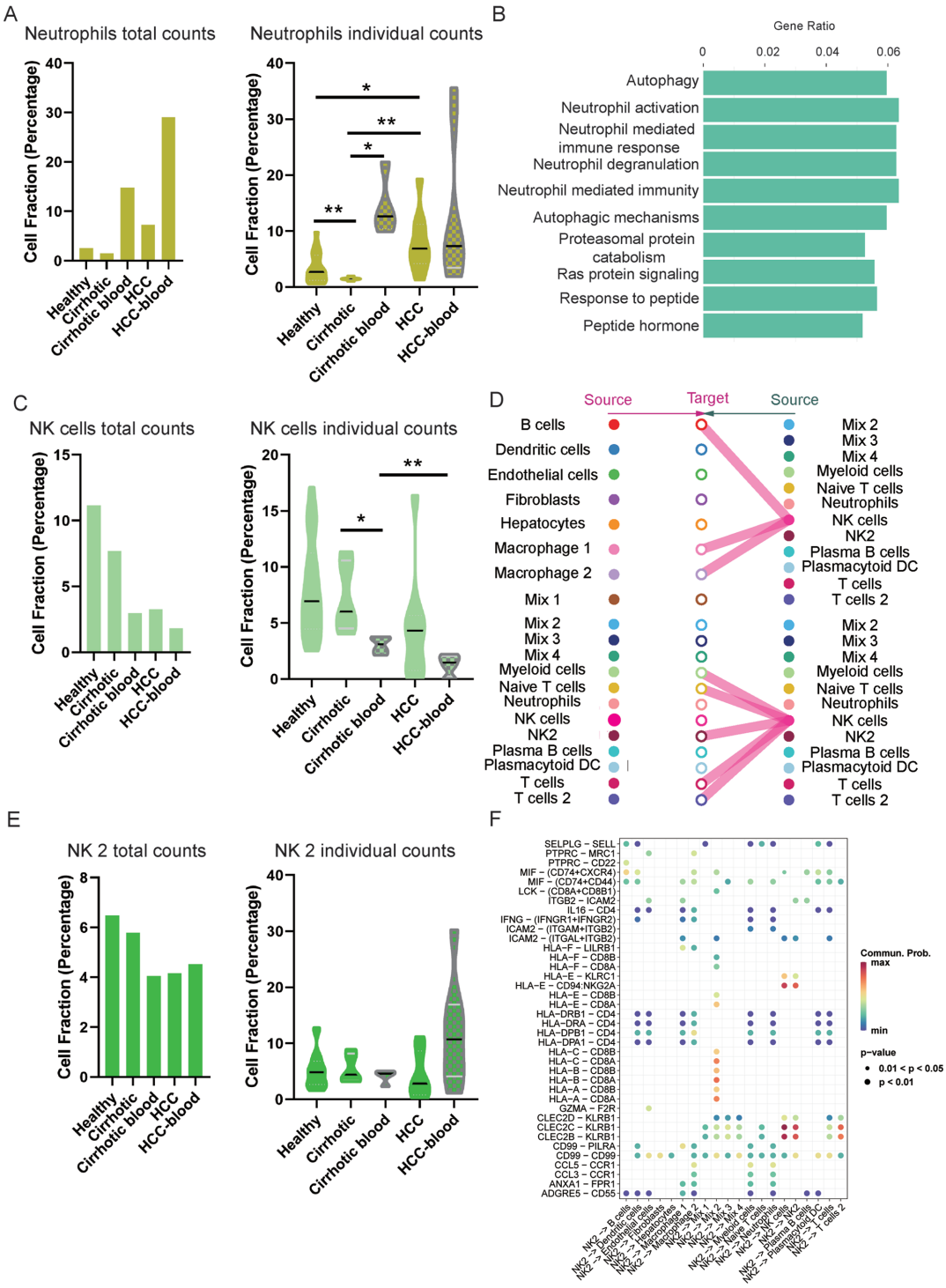

Fig. 3. Distribution of neutrophils and natural killer cells in the tissue and blood samples. (A) Percentages of neutrophils in healthy liver samples, cirrhotic liver samples, cirrhotic blood samples, hepatocellular carcinoma (HCC) tissue samples, and HCC blood samples were calculated. The bar chart (left panel) shows the percentage of neutrophils in all cells (all patients pulled together). The violin plot (right) shows the percentage of neutrophils in each patient. The shape of the violin plot indicates the distribution of data points, lines denote mean and interquartile range. Significance was determined by *t*-test or Wilcoxon's test depending on the results of normality tests and F tests. ***$p<0.001$, **$p<0.01$, *$p<0.05$, ns, not significant ($p>0.05$). (B) Enrichment analysis showing the pathways and cell functions impacted by the differentially expressed genes of the neutrophil cluster. (C) As in (A), but for natural killer (NK) cells. (D) Hierarchical plot shows the inferred intercellular communication network for LIGHT signaling. Circle size is proportional to the number of cells in each cell group and edge width represents the communication probability. Edge colors are consistent with the signaling source, the arrow points from the source to the target. (E) As in (A), but for NK 2 cells. (F) Dot plot showing the signaling patterns of NK2 cells to other cell types. Inferred ligands and receptors are listed. The dot color is proportional to the communication probability computed from pattern recognition analysis. The dot size shows the *p*-value.

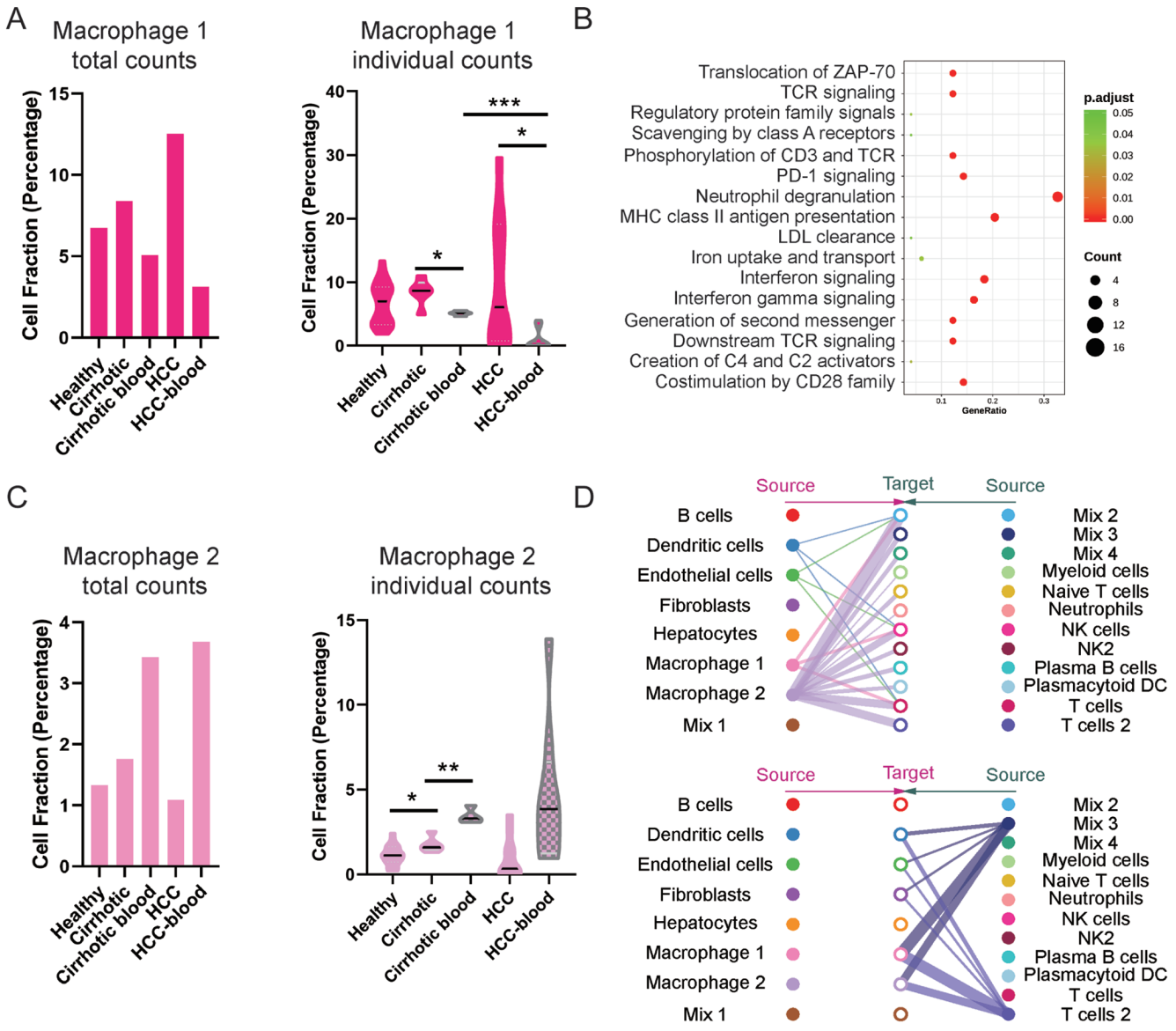

Fig. 4. Two macrophage subsets showed distinct prevalence in cirrhotic tissue or blood samples. (A) Percentages of macrophage 1 in healthy liver samples, cirrhotic liver samples, cirrhotic blood samples, HCC tissue samples, and HCC blood samples were calculated. The bar chart (left panel) shows the percentage of macrophage 1 in all cells (all patients pooled). The violin plot (right) shows the percentage of macrophage 1 in each patient. The shape of the violin plot indicates the distribution of data points, lines denote mean and interquartile range. Statistical difference was compared by t-test or Wilcoxon's test depending on the results of normality tests and F tests. ***p<0.001, **p<0.01, *p<0.05, ns, not significant (p>0.05). (B) Enrichment analysis showing the pathways and cell functions impacted by the differentially expressed genes of the macrophage 1 cluster. (C) As in (A), but for macrophage 2. (D) Hierarchical plot shows the inferred intercellular communication network for CXCL (upper panel) and TNF (lower panel) signaling. Circle sizes are proportional to the number of cells in each cell group and edge width represents the communication probability. Edge colors are consistent with the signaling source, the arrow points from the source to the target. HCC, hepatocellular carcinoma.

than T cells in HCC blood samples (0.81±0.27%). The subset of T cells was involved in p73 transcription factor network, and actively interacted with NK cells (Fig. 2D). Cluster 2 was a second T cell subset (T cell 2) that strongly expressed CD3E, CD2, CD7, and CD69, the percentage of cells expressing CD8 was greater than in cluster 16. The expression of T cell 2 subset showed no clear tissue type preference (Fig. 2E). Functional enrichment analysis showed that these cells were responsible for NFAT signaling, IL5-mediated signaling, CD40/CD40L signaling, and NF-kappa B pathways (Fig. 2F). Given the above, anti-inflammatory T cells were evenly distributed in all sample types, but naïve and memory T cells were depleted in HCC tissue sample and high in blood samples from HCC patients.

Neutrophils were scarce in cirrhotic tissue samples

Neutrophils account for up to 80% of white blood cells in the circulation and around 35–50% of total lymphocytes in the liver.[28] Neutrophils were significantly enriched in cirrhotic blood samples (14.39±2.75%) compared with cirrhotic tissue samples (1.50±0.15%; Fig. 3A). However, the percentages of neutrophils in HCC tissue samples (7.96±1.80%) and HCC blood samples (12.47±4.60%) were similar. In fact, HCC tissues had significantly increased neutrophil infil-

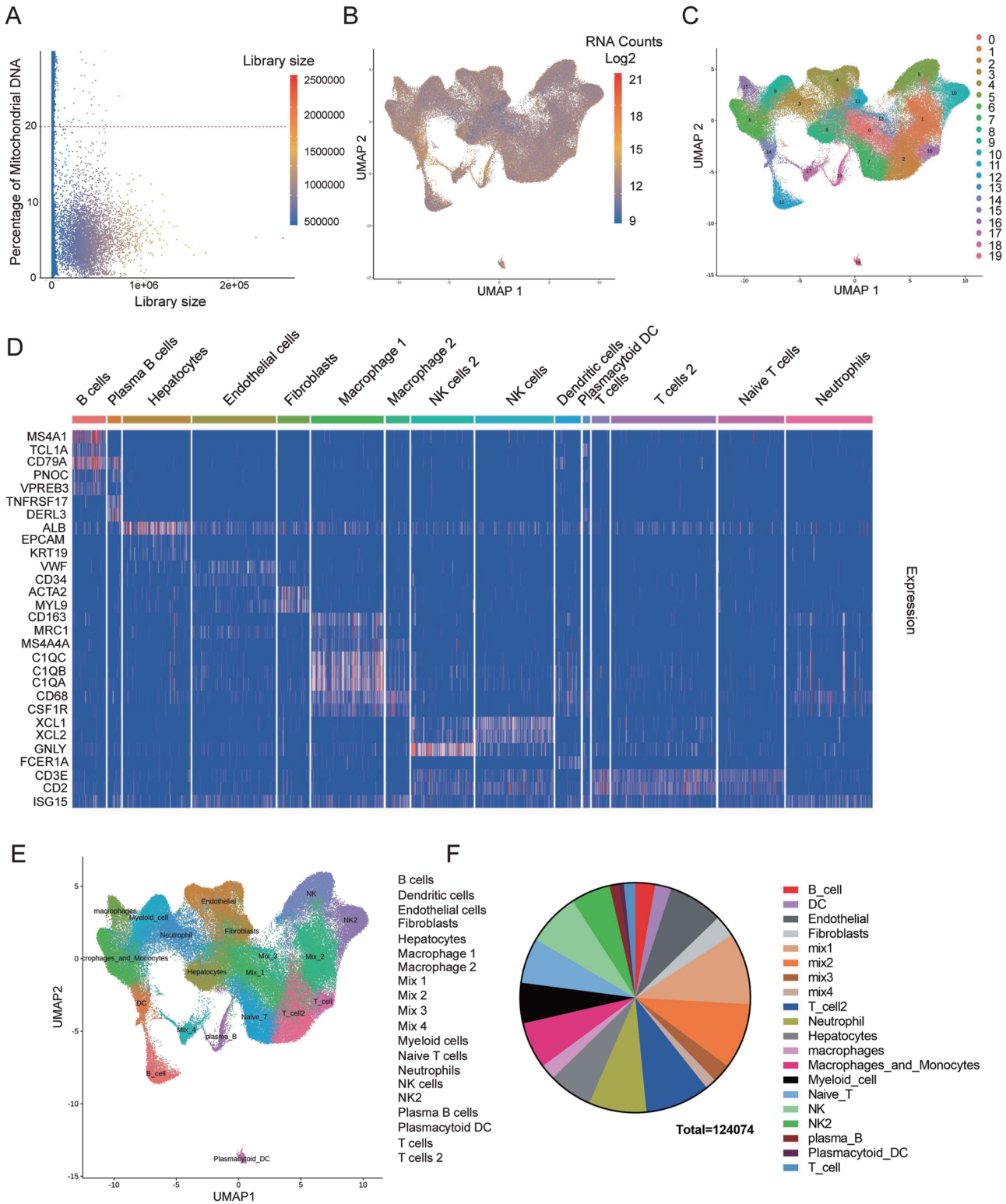

Fig. 5. Immune cell subsets were identified in healthy liver, cirrhotic liver, hepatocellular carcinoma, and peripheral blood samples. (A) Viable cells were filtered from the single cell datasets by selecting cells with the library size of minimum 500 transcripts per cell and a maximum of 70% mitochondrial transcript content. (B) UMAP (uniform manifold approximation and projection) of 124,074 cells, each point represents a single cell. Library size is indicated by color. (C) UMAP showing the results of clustering analysis. Cells exhibiting similar transcriptome profiles were grouped, and the groups were color coded. (D) Expression of marker genes used for the identification of clusters shown in a heatmap. (E) Cluster map showing the assigned identity for each cluster. The X and Y axis labeled uniform approximation of the manifold, showing a nonlinear projection of the reduced dimension. (F) Cell-type composition shown as a pie chart.

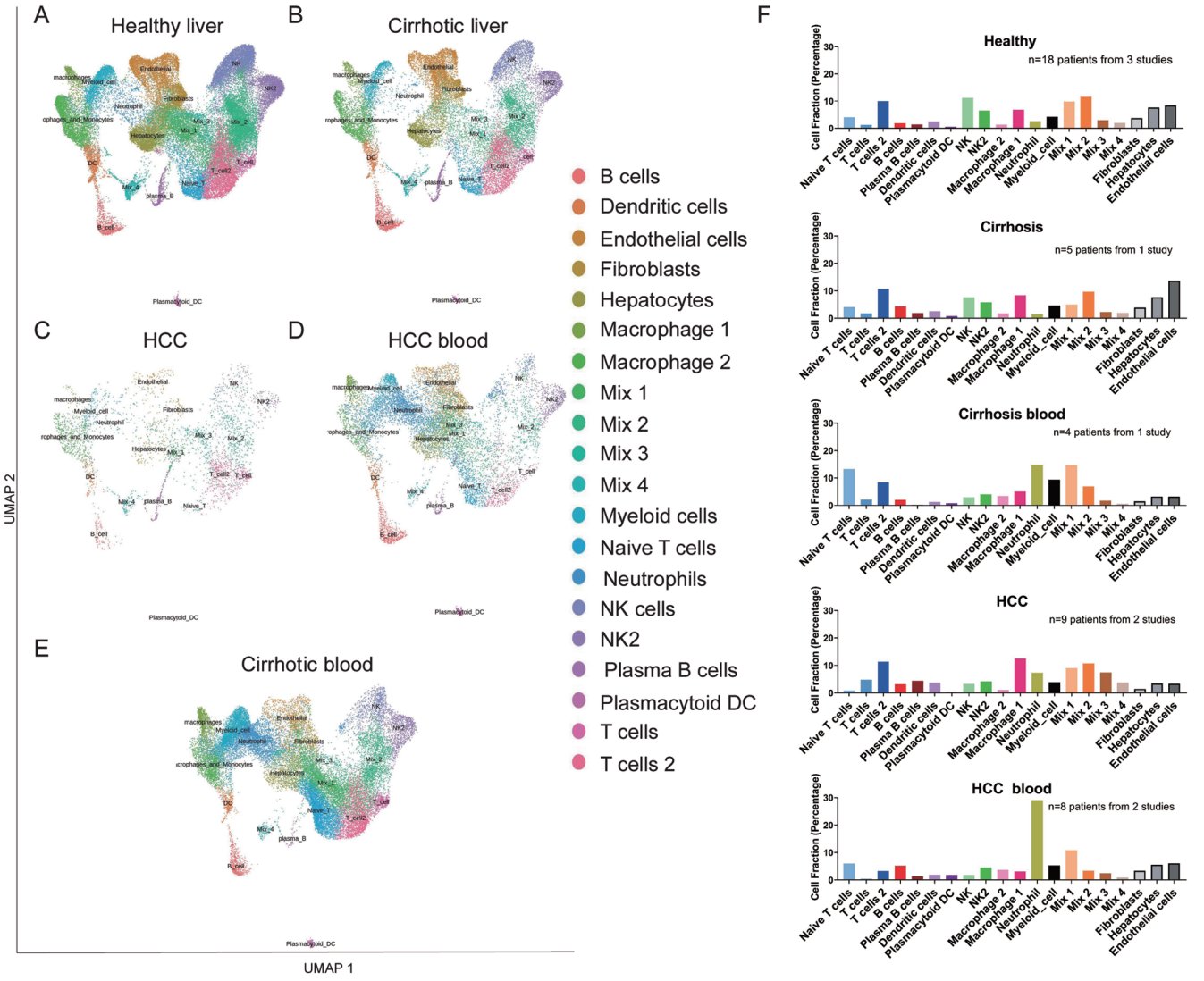

Fig. 6. Healthy liver, cirrhotic liver, hepatocellular carcinoma, peripheral blood of cirrhotic patients, and peripheral blood of hepatocellular carcinoma patients displayed varied immune cell composition. Cluster map showing the assigned identity for each cluster in healthy liver samples. The X and Y axis labeled uniform approximation of the manifold, showing a nonlinear projection of the reduced dimension. (B) As in (A), but for cirrhotic liver samples. (C) As in (A), but for hepatocellular carcinoma (HCC) tissue samples. (D) As in (A), but for peripheral blood samples of cirrhotic patients. (E) As in (A), but for HCC blood samples. (F) Cell fraction of each cell cluster in healthy liver samples, cirrhotic liver samples, HCC tissue samples, HCC blood samples,and cirrhotic blood samples.

tration compared with both healthy (3.49±0.64%) and cirrhotic tissue samples, and neutrophil infiltration in cirrhotic tissue samples was decreased. Enrichment analysis of the DE genes revealed neutrophil activation, neutrophil mediated immunity, and TGF-beta signaling functions (Fig. 3B).

A subset of NK cells was enriched in cirrhotic tissue samples compared with peripheral blood samples

Two NK cell subsets were identified. Cluster 5 (NK) strongly expressed CD7, NKG7, XCL1, XCL2, and cluster 10 (NK2) strongly expressed CD7, GNLY, and NKG7. Neither the NK nor the NK2 clusters were differentially distributed in healthy, cirrhotic, and HCC tissue samples (Fig. 3C–E). However, the NK cluster was significantly enriched in tissue samples compared with blood samples but not in the NK2 cluster (Fig. 3E). The NK cell cluster was involved in canonical cancer signaling, NK cell mediated cytotoxicity, and cell adhesion. It actively interacted with B cells, T cells and macrophages via the LIGHT signaling pathway (Fig. 3D). In comparison, the NK2 cluster was enriched in genes involved in the G2/M checkpoint, and was believed to modulate the mixed cell cluster via HLA-CD8 signaling (Fig. 3F). The immune-active NK cell subset was enriched in tissue samples, but the quiescent NK2 cluster displayed relatively equal distribution.

Pathological tissue samples and blood samples were dominated by distinct macrophage subsets

Two populations of macrophages and monocytes were identified by CD68 expression. Cluster 6 highly expressed CD68, CSF1R, MARCO, C1QA, CD14, and C1QB, whereas cluster 15 was marked by CD68, CSF1R, and MACRO expression, with limited expression of C1QA and C1QB. Cluster 6 (macrophage 1) is a subset of macrophages mixed with a few monocytes that actively interact with T cells and B cells. The

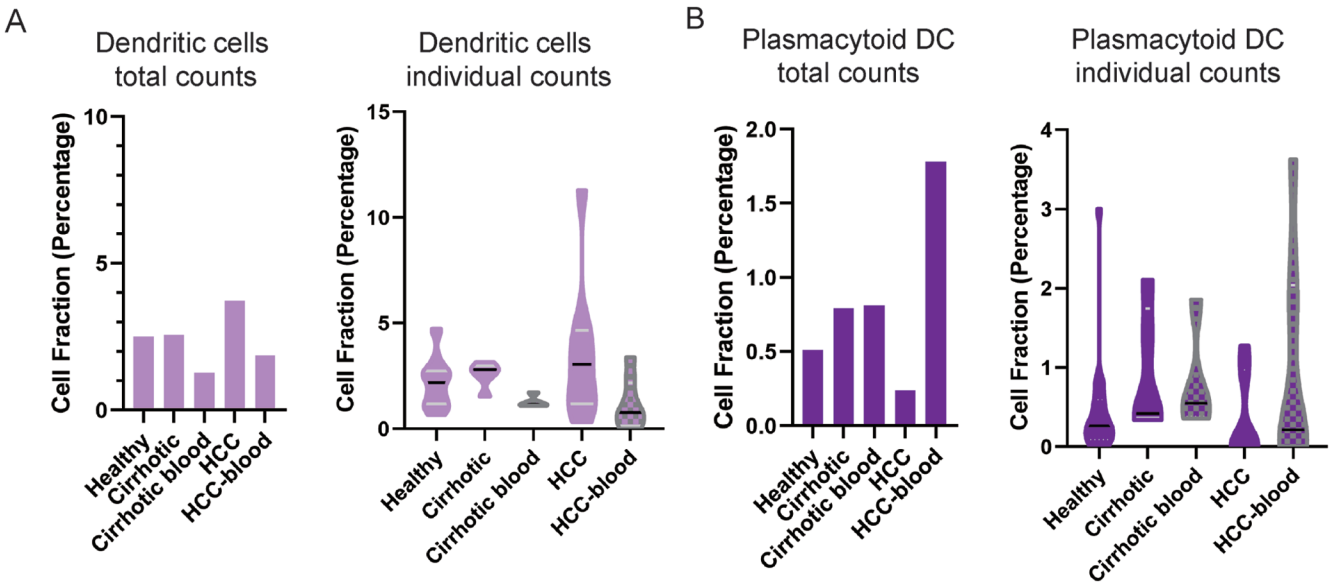

Fig. 7. Dendritic cells were non-differentially observed in all sample types. (A) Percentages of DCs in healthy liver samples, cirrhotic liver samples, cirrhotic blood samples, HCC tissue samples, and HCC blood samples were calculated. The bar chart (left panel) shows the percentage of DCs in all cells (all patients pulled together). The violin plot (right) shows the percentage of DCs in each patient. The shape of the violin plot indicates the distribution of data points, lines denote mean and interquartile range. Significant difference was determined by *t*-test or Wilcoxon's test depending on the results of normality tests and F tests. (B) As in (A), but for plasmacytoid DCs. DCs, dendritic cells; HCC, hepatocellular carcinoma.

infiltration of macrophage 1 cells that actively interact with other immune cells was decreased in blood samples compared with tissue samples (Fig. 4A). In addition, the macrophage population was significantly more enriched in cirrhotic blood samples (5.11±0.18%) compared with HCC blood samples (0.97±0.60%). Enrichment analysis of DEGs pointed to T cell activation, Th1/Th2 differentiation, antigen dependent B-cell activation, TCR signaling, and MHC class II antigen presentation (Fig. 4B).

Cluster 15 (macrophage 2) was characterized by strong expression of LST1, MS4A7, CKB, CDKN1C, RHOC, COTL1, FCER1G, FCGR3A, SAT1, FTH1, and LYN. In contrast to macrophage 1, this macrophage population was more enriched in blood samples than in tissue samples (1.77±0.21% vs 3.44±0.22% for cirrhotic samples, $p<0.01$; 1.05±0.43% vs 4.66±1.52% for HCC samples, not significant; Fig. 4C). The DEGs were involved in NF-kB signaling, TNF-related signaling and toll-like receptor signaling, macrophage 2 actively interacts with T cells (Fig. 4D). Notably, toll-like receptor signaling is required for immune activation.[29] Both macrophage subsets were more prevalent in cirrhotic samples than in healthy and HCC samples.

DCs were enriched in cirrhotic patients with alcoholic liver disease (ALD) and primary biliary cholangitis (PBC)

We identified a DC population and a plasmacytoid DC population based on the expression of FCER1A. Cluster 14 (DC) strongly expressed CD1C, FCER1A, NDRG2, PKIB, CD1E, and CYP2S1, and cluster 19 strongly expressed PACSIN1, DNASE1L3, CLEC4C, LRRC26, SCT, and LAMP5. Unlike other immune cell types, both the DC and plasmacytoid DC populations were not differentially distributed in any sample type (Fig. 7). The expression of genes involved in oxidative stress and the regulation of RHO GTPase was increased in the DC population. The plasmacytoid DC was associated with IL2 signaling events mediated by PIK3.

Next, we investigated the effects of virus infection, tumor staging, or etiology on immune cell infiltration (Fig. 8A). For HCC patients, we grouped the samples by HBV infection status or tumor staging, and compared immune cell infiltration between the groups. To our surprise, none of the differences between the groups of immune cell types were statistically significant (Supplementary Fig. 3). We then grouped liver cirrhosis patients by their etiologies. Interestingly, DCs were relatively more enriched in patients with ALD and PBC than in patients with nonalcoholic fatty liver disease (NAFLD) or hereditary haemochromatosis ($p=0.086$), but the differences were not statistically significant (Fig. 8B). Similarly, healthy individuals with or without Epstein-Barr virus (EBV) or cytomegalovirus (CMV) were compared for changes in their immune landscapes. None of the differences in immune cell types in the EBV positive/negative groups, or CMV positive/negative groups were significant (Supplementary Fig. 4). However, it should be noted that the lack of statistical significance might be the result of the small sample size.

Discussion

The liver is an immunologically active organ that harbors a diverse immune cell repertoire.[30] The balance between immune-tolerance and inflammatory response is crucial to liver function. Immune deficiency may lead to the development of chronic liver disease and cancer. Interpreting the immune microenvironments of healthy and pathological liver provides insights into the change of immune status caused by the diseases, and might guide the design of clinical treatment plans in the future. By integrating and re-analyzing public scRNAseq data, we compared the immune microenvironment of healthy, cirrhotic liver, and HCC tumor, as well as in cirrhotic and HCC peripheral blood. Various types of immune cells, hepatocytes, endothelial cells, and fibroblasts were identified in healthy liver as previously described.[7] T cells, NK cells, and macrophages were the most abundant immune

A

Summary of sample pathology and etiology

Sample ID	Pathology	HBV Infection	Tumor stage	Cirrhosis Etiology	Serologies
S3	HCC	+	I		
S4	HCC	+	II		
S7	HCC	+	IIIA		
S8	HCC	-	IIIA		
S10	HCC	+	IIIA		
S11	HCC	+	IIIA		
S16	LC			NAFLD	
S17	LC			ALD	
S18	LC			ALD	
S19	LC			NAFLD	
S20	LC			PBC	
S21	LC			NAFLD	
S22	LC			Hereditary Haemochromatosis	
S23	LC			NAFLD	
S24	LC			NAFLD	
S25	Healthy				CMV
S26	Healthy				CMV,EBV
S27	Healthy				EBV
S28	Healthy				EBV
S29	Healthy				None

B

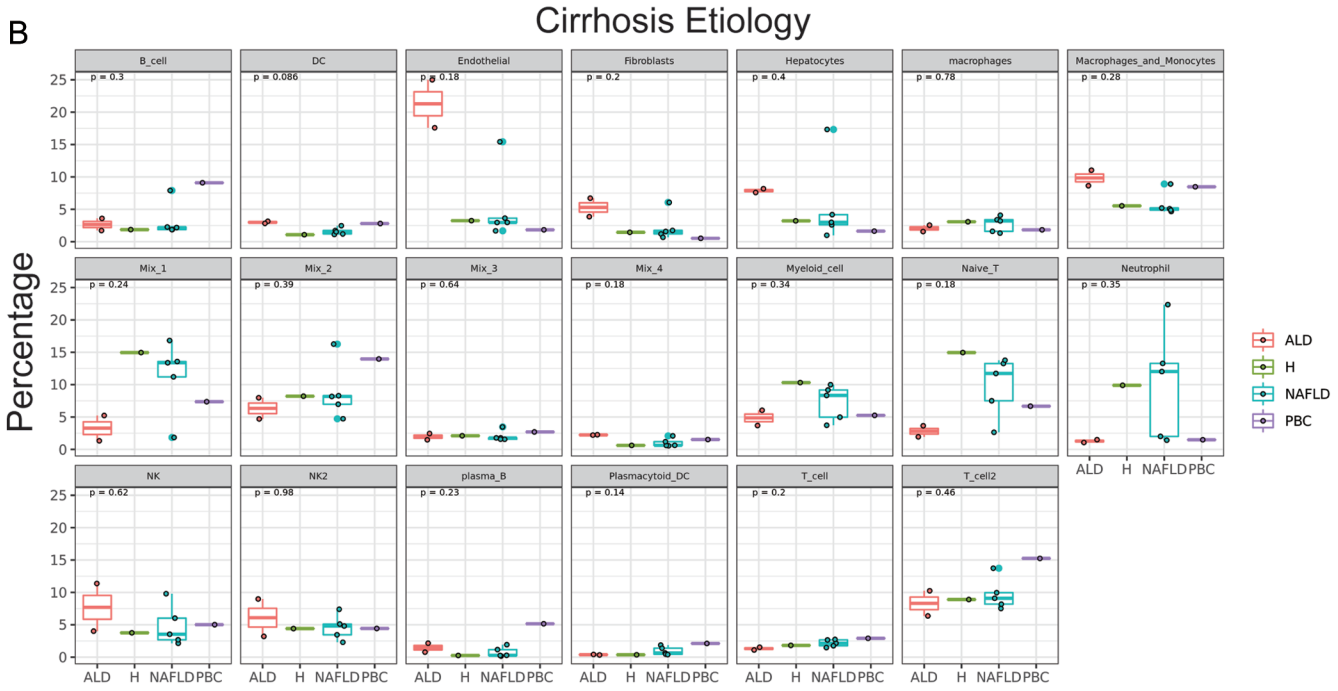

Fig. 8. DCs were enriched in patients suffering from primary biliary cholangitis and alcoholic liver disease. (A) The pathology, HBV infection status, tumor staging, cirrhosis etiology, and serologies of samples were summarized in a table. (B) Immune cell infiltration between ALD (red boxes), hereditary haemochromatosis (green boxes), NAFLD (blue), and PBC (purple) patients were compared by boxplots. Each plot represents one cell type, each dot represents one patient. The data were compared by the Wilcoxon test. HCC, hepatocellular carcinoma; LC, liver cirrhosis; HBV, hepatitis B virus; NAFLD, nonalcoholic fatty liver disease; ALD, alcoholic liver disease; PBC, primary biliary cholangitis; CMV, cytomegalovirus; EBV, Epstein-Barr virus.

cell populations in healthy liver. Interestingly, the abundance of each immune cell type in cirrhotic liver was similar to that of the healthy liver, but the abundance of almost all immune cell types changed greatly in HCC. That observation seems to suggest that the immune microenvironment of cirrhotic liver was not substantially altered, whereas tumorigenesis was strongly associated with the immune microenvironment of the liver. This is to our surprise considering that changes in liver resident microbiome were observed in liver cirrhosis.[31]

In cirrhotic liver, the infiltration of naïve T cells and a subset of macrophages that actively interacts with T cells and B cells were increased. Hepatic T cells exhibited remarkable heterogeneity.[12] Consistently, we identified three T cell subsets, and naïve T cells accumulated in cirrhotic samples. That cluster of cells was positive for both CD4 and CD8, although the expression was relatively low. They displayed poor correlation with cytokine production, as previously described.[32] One study reported that naïve T cells were reduced in liver cirrhosis.[33] However, our study showed that naïve T cells were significantly enriched in cirrhotic tissue samples, but were decreased in HCC samples, indicating a less proinflammatory T cell repertoire in cirrhotic liver.

Two macrophage subsets were identified in this study, however, they had distinct features and cannot be classified as M1 or M2 macrophages based on the expression of gene markers. The CD14 low macrophage 2 was predicted to interact with T cells and B cells, whereas the CD14 high macrophage 1 highly expressed genes for TNF and toll-like receptor signaling. It was postulated that TNF expressing macrophages may interact with T cells and promote T-cell exhaustion, therefore impair antitumor responses and facilitating HCC development.[34] That macrophage subtype was more prevalent in tissue samples than in blood samples, showing that T-cell exhaustion was more evident in local immunity than in peripheral immunity. In contrast, enrichment analysis showed that macrophage 2 up-regulated genes that promote T cell activation, B cell activation, TCR activation, and Th1/Th2 differentiation. Moreover, IL-10 expression was significantly up-regulated in macrophage 2, suggesting an anti-inflammatory role of those cells.[35] Interestingly, the nontypical macrophage subset was significantly increased in cirrhotic samples compared with healthy tissue samples and their abundance was decreased in HCC samples. Given the above, the anti-inflammatory, T cell/B cell interacting macrophage subsets may play a key role in the development of liver cirrhosis.

In contrast, neutrophil infiltration was limited in cirrhotic livers. Neutrophil infiltration, which is required for the antimicrobial immune responses, was observed in varies types of liver disease. However, it was reported that neutrophils were not necessary for establishing chronic inflammation and hepatic fibrosis.[36] Moreover, neutrophils may amplify liver damage. Neutrophil depletion significantly reduced liver damage in an acute liver inflammation mouse model.[37] Neutrophil extracellular traps were shown to disturb hepatic blood flow, which results in mild hepatic injury.[38] Whether neutrophil infiltration promotes liver cirrhosis is under debate, but a study showed that the neutrophil-to-lymphocyte ratio would predict the survival of patients with liver cirrhosis.[39] The mean neutrophil-to-lymphocyte ratio was lower in the survivor group, suggesting that low neutrophil content may benefit patient survival.

In HCC tumors, neutrophil infiltration was significantly increased, which suggests a different role of neutrophil in HCC. Increased neutrophil infiltration has been observed in various cancers, and promotes or suppresses tumorigenesis depending on the local immune microenvironment.[40] Neutrophils were shown to promote cancer cell adhesion to hepatic sinusoids and facilitate cancer invasion.[41] In fact, functional enrichment analysis of the neutrophil cluster identified in our study confirmed their role in promoting cell adhesion. Therefore, neutrophils may be protumorigenic in HCC, and the net neutrophil complement increase may be an indicator of HCC emergence in cirrhotic patients. On the other hand, the proportion of naïve T cells was decreased. Decrease of the quiescent and immune-inactive T cell population was accompanied by the increase of CD4+ and CD8+ T cells, demonstrating a more immune-active microenvironment compared to cirrhotic and healthy liver.

In clinical practice, collecting cirrhotic liver samples for the prediction of HCC is not practical. Therefore, biomarkers by liquid biopsy should be the focus of future research. Comparing the blood samples and tissue samples, it was evident that the immune cell infiltration of the blood sample cannot represent the microenvironment of the tissue samples. The major difference between the cirrhotic and HCC blood sample was manifested by two B cell subsets, T cells, NK cells, and macrophage 1. However, the differences were not observed in tissue samples, indicating that peripheral immunity was more evidently altered, and such changes in immune cells may serve as indicators of HCC development in patients with cirrhosis. Collectively, the dynamics of the immune cell subsets can be considered as novel biomarkers to predict the transition from cirrhosis to HCC.

The main study limitation is that bioinformatics analysis has limited clinical application. More stringent data needs to be shown in terms of bioinformatics approach to be supported. Therefore, prospective clinical studies are required to further validate the conclusions. The immune landscapes of cirrhosis patients with or without HCC development should also be investigated in future studies.

Conclusion

To conclude, marked differences between the tumor-infiltrating lymphocytes in HCC and cirrhotic liver were observed. Decreased naïve T-cell infiltration and increased neutrophil infiltration in the liver may indicate the development of HCC in cirrhotic patients. Decreased infiltration of subsets of macrophages, NK cells, and T cells together with the increase of B cells in the blood may also be the sign of HCC development in cirrhotic patients. The alteration in hepatic immune landscape indicated that the changes in tissue-resident immune cells may serve as the predictor of HCC development. Such alterations in immune cell abundance were also observed in blood samples, suggesting that the surveillance of the development of HCC in cirrhotic patients can be achieved by liquid biopsy. Therefore, it might be plausible that we may prevent the development of HCC by interfering with the modification to the microenvironment of the liver.

Acknowledgments

We thank Dr. Yan Yin for proof reading.

Funding

This study received financial support from the Key-Area Research and Development Program of Guangdong Province (No. 2021B0101420006), the National Natural Science Foundation of China (Nos. 62201557, U20A20171, 121 26608, 82073090), the Shenzhen Science and Technology Innovation Committee Technical Research Projects (Nos. JSGG20180703164202084, KQJSCX20180330124428928, JSGG20180508152646606), the Guangdong Basic and Ap-

plied Basic Research Foundation (Nos. 2020B1515120046, 2021A1515110585), and Shanxi Province "136" Revitalization Medical Project Construction Funds.

Conflict of interest

Yingqiang Li, Yingmei Li, Tianhao Mu and Shifu Chen were employed by HaploX Biotechnology. The other authors have no conflict of interests related to this publication.

Author contributions

Contributed equally to this work (JD, PZ, YZ), study concept and design (JD, PZ, YZ, LZ, SC, ZL), acquisition of data (JD, YL, SC), analysis and interpretation of data (JD, PZ, YZ, LZ, SC, ZL, YL), administrative, technical, or material support (LZ, SC), and study supervision (LZ, SC, ZL). All authors made significant contributions to this study and approved the final manuscript. All authors were involved in the design and drafting of the manuscript. All authors approved the manuscript.

Data sharing statement

RNA sequencing data used in this study were downloaded from the GEO database and BIG data center under the access numbers of SRP073767, GSE115469, GSE136103, GSE124395, GSE107747, and HRA000069.

References

[1] Sung H, Ferlay J, Siegel RL, Laversanne M, Soerjomataram I, Jemal A, *et al*. Global Cancer Statistics 2020: GLOBOCAN Estimates of Incidence and Mortality Worldwide for 36 Cancers in 185 Countries. CA Cancer J Clin 2021; 71(3):209–249. doi:10.3322/caac.21660, PMID:33538338.
[2] Fattovich G, Stroffolini T, Zagni I, Donato F. Hepatocellular carcinoma in cirrhosis: incidence and risk factors. Gastroenterology 2004;127(5 Suppl 1):S35–50. doi:10.1053/j.gastro.2004.09.014, PMID:15508101.
[3] Ramakrishna G, Rastogi A, Trehanpati N, Sen B, Khosla R, Sarin SK. From cirrhosis to hepatocellular carcinoma: new molecular insights on inflammation and cellular senescence. Liver Cancer 2013;2(3-4):367–383. doi:10.1159/000343852, PMID:24400224.
[4] Shan S, Chen W, Jia JD. Transcriptome Analysis Revealed a Highly Connected Gene Module Associated With Cirrhosis to Hepatocellular Carcinoma Development. Front Genet 2019;10:305. doi:10.3389/fgene.2019.00305, PMID:31001331.
[5] Jiang M, Zeng Q, Dai S, Liang H, Dai F, Xie X, *et al*. Comparative analysis of hepatocellular carcinoma and cirrhosis gene expression profiles. Mol Med Rep 2017;15(1):380–386. doi:10.3892/mmr.2016.6021, PMID:27959423.
[6] Muller M, Bird TG, Nault JC. The landscape of gene mutations in cirrhosis and hepatocellular carcinoma. J Hepatol 2020;72(5):990–1002. doi:10.1016/j.jhep.2020.01.019, PMID:32044402.
[7] Aizarani N, Saviano A, Sagar, Mailly L, Durand S, Herman JS, *et al*. A human liver cell atlas reveals heterogeneity and epithelial progenitors. Nature 2019; 572(7768):199–204. doi:10.1038/s41586-019-1373-2, PMID:31292543.
[8] Zhang Q, He Y, Luo N, Patel SJ, Han Y, Gao R, *et al*. Landscape and Dynamics of Single Immune Cells in Hepatocellular Carcinoma. Cell 2019;179(4):829–845.e820. doi:10.1016/j.cell.2019.10.003, PMID:31675496.
[9] MacParland SA, Liu JC, Ma XZ, Innes BT, Bartczak AM, Gage BK, *et al*. Single cell RNA sequencing of human liver reveals distinct intrahepatic macrophage populations. Nat Commun 2018;9(1):4383. doi:10.1038/s41467-018-06318-7, PMID:30348985.
[10] Ramachandran P, Dobie R, Wilson-Kanamori JR, Dora EF, Henderson BEP, Luu NT, *et al*. Resolving the fibrotic niche of human liver cirrhosis at single-cell level. Nature 2019;575(7783):512–518. doi:10.1038/s41586-019-1631-3, PMID:31597160.
[11] D'Avola D, Villacorta-Martin C, Martins-Filho SN, Craig A, Labgaa I, von Felden J, *et al*. High-density single cell mRNA sequencing to characterize circulating tumor cells in hepatocellular carcinoma. Sci Rep 2018;8(1):11570. doi:10.1038/s41598-018-30047-y, PMID:30068984.
[12] Zheng C, Zheng L, Yoo JK, Guo H, Zhang Y, Guo X, *et al*. Landscape of Infiltrating T Cells in Liver Cancer Revealed by Single-Cell Sequencing. Cell 2017;169(7):1342–1356.e1316. doi:10.1016/j.cell.2017.05.035, PMID:28622514.
[13] Zheng GX, Terry JM, Belgrader P, Ryvkin P, Bent ZW, Wilson R, *et al*. Massively parallel digital transcriptional profiling of single cells. Nat Commun 2017;8:14049. doi:10.1038/ncomms14049, PMID:28091601.
[14] Stuart T, Butler A, Hoffman P, Hafemeister C, Papalexi E, Mauck WM 3rd, *et al*. Comprehensive Integration of Single-Cell Data. Cell 2019;177(7):1888–1902.e1821. doi:10.1016/j.cell.2019.05.031, PMID:31178118.
[15] Trapnell C, Cacchiarelli D, Grimsby J, Pokharel P, Li S, Morse M, *et al*. The dynamics and regulators of cell fate decisions are revealed by pseudotemporal ordering of single cells. Nat Biotechnol 2014;32(4):381–386. doi:10.1038/nbt.2859, PMID:24658644.
[16] Aran D, Looney AP, Liu L, Wu E, Fong V, Hsu A, *et al*. Reference-based analysis of lung single-cell sequencing reveals a transitional profibrotic macrophage. Nat Immunol 2019;20(2):163–172. doi:10.1038/s41590-018-0276-y, PMID:30643263.
[17] Yu G, Wang LG, Han Y, He QY. clusterProfiler: an R package for comparing biological themes among gene clusters. OMICS 2012;16(5):284–287. doi:10.1089/omi.2011.0118, PMID:22455463.
[18] Ashburner M, Ball CA, Blake JA, Botstein D, Butler H, Cherry JM, *et al*. Gene ontology: tool for the unification of biology. The Gene Ontology Consortium. Nat Genet 2000;25(1):25–29. doi:10.1038/75556, PMID:10802651.
[19] Ogata H, Goto S, Sato K, Fujibuchi W, Bono H, Kanehisa M. KEGG: Kyoto Encyclopedia of Genes and Genomes. Nucleic Acids Res 1999;27(1):29–34. doi:10.1093/nar/27.1.29, PMID:9847135.
[20] Jin S, Guerrero-Juarez CF, Zhang L, Chang I, Ramos R, Kuan CH, *et al*. Inference and analysis of cell-cell communication using CellChat. Nat Commun 2021;12(1):1088. doi:10.1038/s41467-021-21246-9, PMID:33597522.
[21] Kourea H, Kotoula V. Towards tumor immunodiagnostics. Ann Transl Med 2016;4(14):263. doi:10.21037/atm.2016.07.07, PMID:27563650.
[22] Minnema-Luiting J, Vroman H, Aerts J, Cornelissen R. Heterogeneity in Immune Cell Content in Malignant Pleural Mesothelioma. Int J Mol Sci 2018;19(4):1041. doi:10.3390/ijms19041041, PMID:29601534.
[23] Impola U, Larjo A, Salmenniemi U, Putkonen M, Itala-Remes M, Partanen J. Graft Immune Cell Composition Associates with Clinical Outcome of Allogeneic Hematopoietic Stem Cell Transplantation in Patients with AML. Front Immunol 2016;7:523. doi:10.3389/fimmu.2016.00523, PMID:27917176.
[24] Lyons YA, Wu SY, Overwijk WW, Baggerly KA, Sood AK. Immune cell profiling in cancer: molecular approaches to cell-specific identification. NPJ Precis Oncol 2017;1(1):26. doi:10.1038/s41698-017-0031-0, PMID:29872708.
[25] Danaher P, Warren S, Dennis L, D'Amico L, White A, Disis ML, *et al*. Gene expression markers of Tumor Infiltrating Leukocytes. J Immunother Cancer 2017;5:18. doi:10.1186/s40425-017-0215-8, PMID:28239471.
[26] Papalexi E, Satija R. Single-cell RNA sequencing to explore immune cell heterogeneity. Nat Rev Immunol 2018;18(1):35–45. doi:10.1038/nri.2017.76, PMID:28787399.
[27] Zhang X, Lan Y, Xu J, Quan F, Zhao E, Deng C, *et al*. CellMarker: a manually curated resource of cell markers in human and mouse. Nucleic Acids Res 2019;47(D1):D721–D728. doi:10.1093/nar/gky900, PMID:30289549.
[28] Klugewitz K, Adams DH, Emoto M, Eulenburg K, Hamann A. The composition of intrahepatic lymphocytes: shaped by selective recruitment? Trends Immunol 2004;25(11):590–594. doi:10.1016/j.it.2004.09.006, PMID:15489187.
[29] Matsumura T, Ito A, Takii T, Hayashi H, Onozaki K. Endotoxin and cytokine regulation of toll-like receptor (TLR) 2 and TLR4 gene expression in murine liver and hepatocytes. J Interferon Cytokine Res 2000;20(10):915–921. doi:10.1089/10799900050163299, PMID:11054280.
[30] Kubes P, Jenne C. Immune Responses in the Liver. Annu Rev Immunol 2018;36:247–277. doi:10.1146/annurev-immunol-051116-052415, PMID:29328785.
[31] Qin N, Yang F, Li A, Prifti E, Chen Y, Shao L, *et al*. Alterations of the human gut microbiome in liver cirrhosis. Nature 2014;513(7516):59–64. doi:10.1038/nature13568, PMID:25079328.
[32] van den Broek T, Borghans JAM, van Wijk F. The full spectrum of human naive T cells. Nat Rev Immunol 2018;18(6):363–373. doi:10.1038/s41577-018-0001-y, PMID:29520044.
[33] Lario M, Munoz L, Ubeda M, Borrero MJ, Martinez J, Monserrat J, *et al*. Defective thymopoiesis and poor peripheral homeostatic replenishment of T-helper cells cause T-cell lymphopenia in cirrhosis. J Hepatol 2013;59(4):723–730. doi:10.1016/j.jhep.2013.05.042, PMID:23742913.
[34] Dou L, Shi X, He X, Gao Y. Macrophage Phenotype and Function in Liver Disorder. Front Immunol 2019;10:3112. doi:10.3389/fimmu.2019.03112, PMID:32047496.
[35] Thompson K, Maltby J, Fallowfield J, McAulay M, Millward-Sadler H, Sheron N. Interleukin-10 expression and function in experimental murine liver inflammation and fibrosis. Hepatology 1998;28(6):1597–1606. doi:10.1002/hep.510280620, PMID:9828224.
[36] O'Brien KM, Allen KM, Rockwell CE, Towery K, Luyendyk JP, Copple BL. IL-17A synergistically enhances bile acid-induced inflammation during obstructive cholestasis. Am J Pathol 2013;183(5):1498–1507. doi:10.1016/j.ajpath.2013.07.019, PMID:24012680.
[37] Moles A, Murphy L, Wilson CL, Chakraborty JB, Fox C, Park EJ, *et al*. A TLR2/S100A9/CXCL-2 signaling network is necessary for neutrophil recruitment in acute and chronic liver injury in the mouse. J Hepatol 2014;60(4):782–791. doi:10.1016/j.jhep.2013.12.005, PMID:24333183.
[38] Bukong TN, Cho Y, Iracheta-Vellve A, Saha B, Lowe P, Adejumo A, *et al*. Abnormal neutrophil traps and impaired efferocytosis contribute to liver injury and sepsis severity after binge alcohol use. J Hepatol 2018;69(5):1145–1154. doi:10.1016/j.jhep.2018.07.005, PMID:30030149.
[39] Biyik M, Ucar R, Solak Y, Gungor G, Polat I, Gaipov A, *et al*. Blood neutrophil-to-lymphocyte ratio independently predicts survival in patients with liver cirrhosis. Eur J Gastroenterol Hepatol 2013;25(4):435–441. doi:10.1097/MEG.0b013e32835c2af3, PMID:23249602.
[40] Xu R, Huang H, Zhang Z, Wang FS. The role of neutrophils in the development of liver diseases. Cell Mol Immunol 2014;11(3):224–231. doi:10.1038/cmi.2014.2, PMID:24633014.
[41] McDonald B, Spicer J, Giannais B, Fallavollita L, Brodt P, Ferri LE. Systemic inflammation increases cancer cell adhesion to hepatic sinusoids by neutrophil mediated mechanisms. Int J Cancer 2009;125(6):1298–1305. doi:10.1002/ijc.24409, PMID:19431213.